Brain Advance Access published November 25, 2015

BRAIN
A JOURNAL OF NEUROLOGY

REPORT

Early detection of intentional harm in the human amygdala

Eugenia Hesse,[1,2,3,*] Ezequiel Mikulan,[1,2,4,*] Jean Decety,[5] Mariano Sigman,[6,7] María del Carmen Garcia,[8] Walter Silva,[8] Carlos Ciraolo,[8] Esteban Vaucheret,[8] Fabricio Baglivo,[1,2,3] David Huepe,[2] Vladimir Lopez,[9] Facundo Manes,[1,2,4,10] Tristan A. Bekinschtein[11] and Agustin Ibanez[1,2,4,10,12]

*These authors contributed equally to this work.

A decisive element of moral cognition is the detection of harm and its assessment as intentional or unintentional. Moral cognition engages brain networks supporting mentalizing, intentionality, empathic concern and evaluation. These networks rely on the amygdala as a critical hub, likely through frontotemporal connections indexing stimulus salience. We assessed inferences about perceived harm using a paradigm validated through functional magnetic resonance imaging, eye-tracking and electroencephalogram recordings. During the task, we measured local field potentials in three patients with depth electrodes ($n = 115$) placed in the amygdala and in several frontal, temporal, and parietal locations. Direct electrophysiological recordings demonstrate that intentional harm induces early activity in the amygdala (<200 ms), which—in turn—predicts intention attribution. The amygdala was the only site that systematically discriminated between critical conditions and predicted their classification of events as intentional. Moreover, connectivity analysis showed that intentional harm induced stronger frontotemporal information sharing at early stages. Results support the 'many roads' view of the amygdala and highlight its role in the rapid encoding of intention and salience—critical components of mentalizing and moral evaluation.

1 Laboratory of Experimental Psychology and Neuroscience, Institute of Cognitive Neurology, Favaloro University, Buenos Aires, Argentina
2 UDP-INECO Foundation Core on Neuroscience (UIFCoN), Faculty of Psychology, Universidad Diego Portales, Santiago, Chile
3 Instituto de Ingeniería Biomédica, Facultad de Ingeniería, Universidad de Buenos Aires, Argentina
4 National Research Council (CONICET), Buenos Aires, Argentina
5 Department of Psychology, and Department of Psychiatry and Behavioural Neuroscience, The University of Chicago, Chicago, IL, USA
6 Laboratory of Neuroscience, Universidad Torcuato Di Tella, Buenos Aires, Argentina
7 Departamento de Física, FCEN, UBA and IFIBA, Conicet, Buenos Aires, Argentina
8 Programa de Cirugía de Epilepsia, Hospital Italiano de Buenos Aires, Buenos Aires, Argentina
9 Escuela de Psicología, Pontificia Universidad Católica de Chile, Santiago, Chile
10 Centre of Excellence in Cognition and its Disorders, Australian Research Council (ARC), New South Wales, Australia
11 Department of Psychology, University of Cambridge, Cambridge, UK
12 Universidad Autónoma del Caribe, Barranquilla, Colombia

Correspondence to: Agustin Ibanez,
Laboratory of Experimental Psychology and Neuroscience,
Institute of Cognitive Neurology,
Favaloro University, Buenos Aires, Argentina
E-mail: aibanez@ineco.org.ar

Keywords: amygdala; intentional harm; moral cognition; intracranial recordings

Abbreviation: wSMI = weighted Symbolic Mutual Information

Received June 16, 2015. Revised September 22, 2015. Accepted September 25, 2015.

Introduction

Perceiving and reacting to harm is crucial for survival and social interaction. Indeed, the assessment of deliberately harmful actions moulds human morality (Decety *et al.*, 2012; Treadway *et al.*, 2014; Ames and Fiske, 2015). Moral evaluation engages neurocognitive mechanisms supporting theory of mind, intentionality, empathic concern and evaluation (Moll *et al.*, 2005; Young *et al.*, 2007; Moll and Schulkin, 2009; Decety and Cowell, 2014). Neuroimaging studies show that these cognitive domains involve widely distributed networks (Moll and Schulkin, 2009; Decety *et al.*, 2012; Ibanez and Manes, 2012). This network relies on the amygdala as a critical hub (Treadway *et al.*, 2014), likely through frontotemporal connections indexing stimulus salience (Pessoa and Adolphs, 2010).

However, available evidence presents various limitations. First, functional MRI studies of morality are blind to early differences among relevant mechanisms (Huebner *et al.*, 2009). Second, amygdala activation is confounded by stimulus-related signal fluctuation in nearby veins draining distant brain regions (Boubela *et al.*, 2015). Third, EEG/MEG studies of subcortical source space are inaccurate. Thus, no evidence exists of a direct and early involvement of the amygdala in the detection of intentional harm.

To bridge these gaps, we assessed inferences about perceived harm using a paradigm previously validated through functional MRI and eye-tracking (Decety *et al.*, 2012) as well as EEG recordings (Decety and Cacioppo, 2012; Escobar *et al.*, 2014). Participants viewed short videos depicting interactive situations that involved intentional harm, unintentional harm or no harm at all. Their task was to evaluate whether the actions were intentional or unintentional. All stimuli were presented in a three-frame sequence (T1: 500 ms, T2: 200 ms, T3: 1000 ms; see 'Materials and methods' section).

Materials and methods

Participants

Three patients with intractable epilepsy who were offered surgical intervention to alleviate their condition took part in the study. Subject 1 was a 19-year-old, right-handed female who had completed 1 year of tertiary education and suffered from drug-resistant epilepsy since the age of 16 years. Subject 2 was a 57-year-old, left-handed male with an undergraduate degree who suffered from drug-resistant epilepsy since the age of 42 years. Subject 3 was a 29-year-old, left-handed female with an undergraduate degree who suffered from epilepsy since the age of 18 years. All of the subjects gave written informed consent in accordance with the Declaration of Helsinki, and the study was approved by the Institutional Ethics Committee of the Hospital Italiano de Buenos Aires, Argentina. They were attentive and cooperative while performing the task. Their cognitive performance under the task was accurate (Supplementary Table 1).

Patients' recordings

Direct cortical recordings were obtained from semi-rigid, multi-lead electrodes that were implanted in each patient. The electrodes used have a diameter of 0.8 mm and consist of 5, 10 or 15 contact leads 2-mm wide and 1.5-mm apart (DIXI Medical Instruments). The video-SEEG monitoring system (Micromed) records as many as 128 depth-EEG electrode sites simultaneously. Our three subjects had electrodes in the left amygdala, although two of them were left-handed. No data were collected from the right amygdala. All patients were carefully selected such that the amygdalae from which the recordings were obtained were distal to the epileptogenic foci, and no single recording site presented epileptogenic activity (see below). Subject 1 had 128 sites recorded. Subject 2 had 90 sites recorded. Subject 3 had 105 sites recorded. The recordings were sampled at 1024 Hz.

Post-implantation MRI and CT scans were obtained from each patient. Both volumetric images were affine registered and normalized using the SPM8 MATLAB toolbox. Using MRIcron, the MNI coordinates of each contact site and their respective Brodmann areas were obtained and are listed in Supplementary Table 2. We used the normalized position of the electrodes' contact sites to an MNI coordinate space because this procedure allowed us to define the patient's results in a common space (Foster *et al.*, 2015).

Experimental design: task and stimuli

We used an adaptation of the Intention Inference Task (Decety *et al.*, 2012; Decety and Cacioppo, 2012; Escobar *et al.*, 2014) to assess the detection of intentional harmful actions. The task evaluates intentional detection in the context of intentional/unintentional/neutral harms and consists of three scenarios: (i) intentional harm in which one person is in a painful situation intentionally caused by another (e.g. pushing someone off a bench); or (ii) unintentional harms in which one person is in a painful situation unintentionally caused by another; and (iii) neutral or control situations (e.g. one person receiving a flower given by another). The Intention Inference Task evaluates the comprehension of the unintentional or deliberate nature of the action and the intention of the perpetrator to hurt. It consists of 25 animated scenarios (11 intentional, 11 unintentional, three neutral), and one practice trial for each category (before the task). The patients were asked to perform the task a few times. Subjects performed the task twice (Subject 2 three times). Although these are a small number of trials, our results were robust and were consistent with the single trial responses observed in intracranial recordings and their enhanced signal-to-noise ratio (Jacobs and Kahana, 2010). Each scenario consists of three digital colour pictures presented in a successive manner to imply motion. The durations of the first, second and third pictures in each animation were 500 (T1), 200 (T2), and 1000 (T3) ms, respectively. See the Supplementary material for stimuli validation with behavioural and eye-tracking measures. For additional stimulus examples and validation information, see Fig. 1A, Supplementary Fig. 1 and Supplementary material. For a video illustration of the clips, see Supplementary Video 1.

The faces of the protagonists were not visible and thus there were no facial emotional reactions visible to the patients. However, body expressions and postures provided sufficient

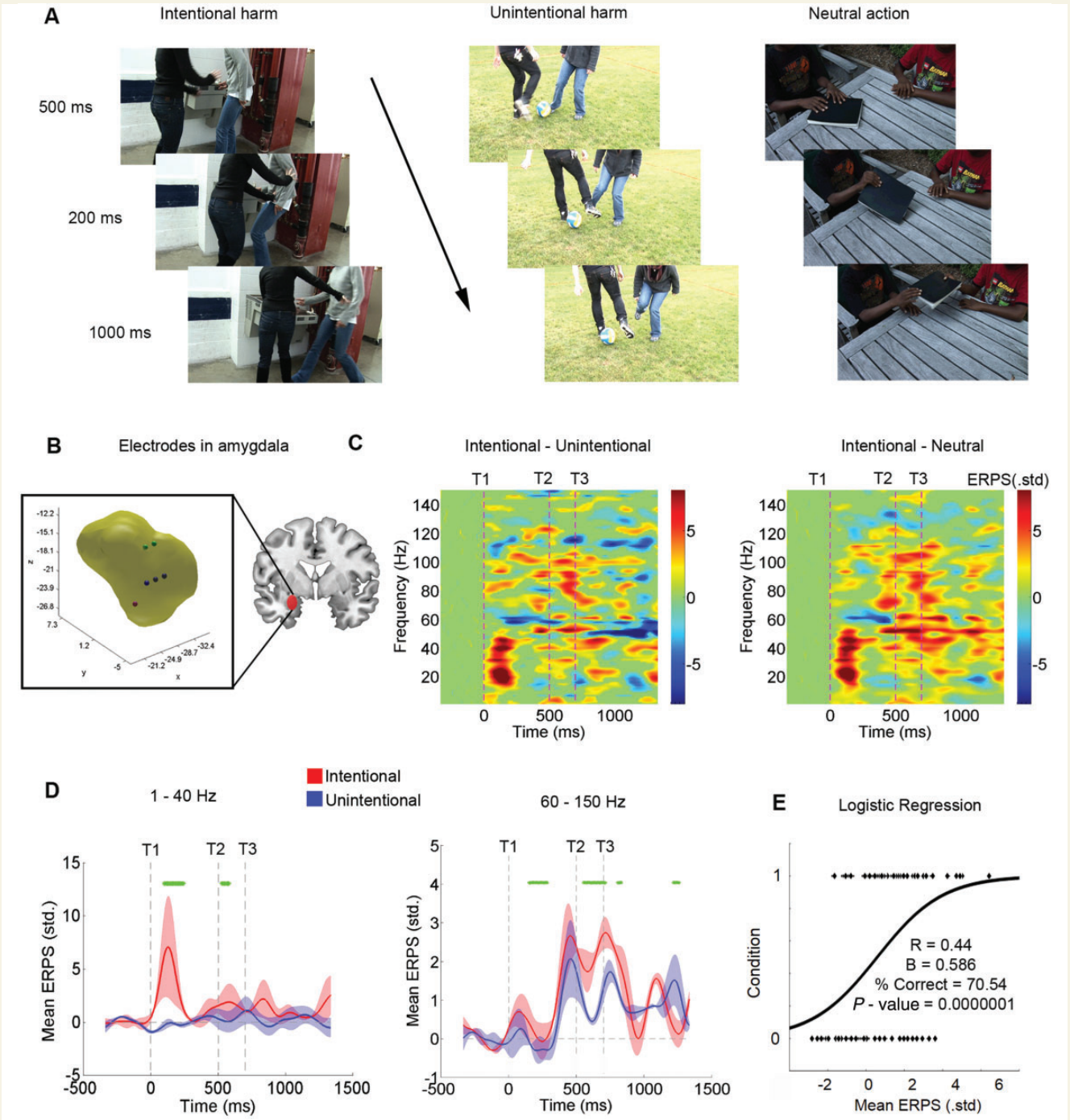

Figure 1 Amygdala responses to intentional harm. (**A**) Examples of stimuli used for intentional, unintentional, and neutral conditions, together with the temporal duration of each image (see examples in Supplementary Video 1). (**B**) Electrode contact sites in the amygdala. (**C**) Time-frequency charts. T1, T2 and T3 represent the times at which each digital picture is presented to the subject. A zero value was assigned to points that were not significant ($P > 0.05$) relative to the baseline. *Left*: Subtraction between the amygdala time-frequency charts obtained from the intentional and unintentional conditions. *Right*: Subtraction between the amygdala time-frequency charts obtained from the intentional and neutral conditions. (**D**) Averaged power spectrum of the intentional and unintentional time-frequency charts using different frequency ranges. The green marks identify significant differences between conditions (bootstrapping, $P < 0.01$). *Left*: Frequency range 1–40 Hz. *Right*: 60–150 Hz. (**E**) Binary logistic regression between conditions (intentional = 1, unintentional = 0) and mean value of the power spectrum on broadband and 0–1000 ms window (B = 0.580, R = 0.44, $P = 0.0000001$, correct categorization = 70.54%).

information about the intention of the agent. Patients were asked to respond to intentionality (was the harmful action done on purpose?). The question was answered by selecting 'Yes' or 'No' with two different buttons.

Data analysis

Signal preprocessing

The data were bandpass filtered from 1 to 200 Hz using a zero phase shift finite impulse filter. Then, they were notch filtered at 50 Hz and its harmonic frequencies (100 Hz, 150 Hz) to eliminate the line artefacts. The contact sites recorded from each patient who presented artefacts and pathological waveforms were discarded. This was achieved by visually inspecting the recordings and by the following criteria: (i) signal values do not exceed five times the signal mean; and/or (ii) consecutive signal samples do not exceed 5 standard deviations (SD) from the gradient mean. A total number of 115 contact sites remained after applying these criteria (35 contact sites for Subject 1, 44 for Subject 2 and 36 for Subject 3; Supplementary Fig. 2).

Once the sites that complied with the criteria were selected, they were referenced to the mean value (the averages of the sites per subject were subtracted from each recording). Finally, the data were segmented into 2000 ms epochs, including a −500 to 0 ms prestimulus baseline period. The epochs were baseline corrected.

Time–frequency analysis

The time–frequency charts were obtained by analysing the digitized signals using a windowed Fourier transform (window length: 250 ms, step 8 ms, window overlap 97%) (Gross, 2014). Our scripts were based on the newtimef.m script. As the frequency analysis is window-centred, we consider that the earliest unbiased significant temporal value is ∼125 ms, when the window centre is at 0 ms (T1 stimulus presentation, see Supplementary material). The time–frequency charts were normalized to the baseline before the stimulus onset. The normalization involved subtracting the baseline average and dividing by the baseline standard deviation on a frequency-by-frequency basis using a window from −500 to 0 relative to the stimuli onset.

We obtained the time–frequency chart for each condition (intentional, unintentional and neutral harmful actions) and performed subtractions between them (intentional − unintentional, intentional − neutral and unintentional − neutral). Significant power increases and decreases across time against baseline values were analysed with Monte Carlo permutation tests (5000) combined with bootstrapping, as reported in other intracranial studies (Naccache *et al.*, 2005; Ibanez *et al.*, 2013). This simple method offers a straightforward solution for multiple comparison problems and for data distribution assumptions. Frequency band ranges of 1 to 40 Hz and broadband (60 to 150 Hz) of the time-frequency charts were averaged for the signals obtained from the intentional and unintentional conditions.

Logistic regression of the trial-by-trial analysis

Logistic regression analysis was performed to evaluate whether the power activity across each trial could predict the subject categorization as intentional or unintentional. The dependent variable was the unintentional (0) or intentional (1) condition. The independent variable of interest was the averaged value of power spectrum over time (0–1000 ms since stimuli onset) for the 60–150 Hz frequency range in each trial. Statistical significance was considered to be $P < 0.01$. Outliers were detected using the Tukey two-sided method (Tukey hinge distance factor = 1.5) (Tukey, 1977). Three outlier values were detected and left out of the analysis. This procedure was done for the amygdala power spectrum values and for the other regions, grouped by regions of interest within subjects (see below).

Comparison between the amygdala and the other regions

To assess the amygdala's power activation and ability to distinguish between conditions (logistic regression) relative to the other regions, we performed a three-step analysis: (i) to evaluate whether the region discriminates the intentional condition, and the intentional from unintentional conditions; (ii) to compare the amygdala's power activation with that of the regions that did discriminate the intentional conditions and the intentional from unintentional conditions; and (iii) to perform a logistic regression of single trial data as predictors of subject classification. See Supplementary material for detailed information on this three-step analysis.

Amygdala connectivity analysis using the weighted Symbolic Mutual Information measure

To analyse the amygdala's connectivity with the other regions within each subject, we used the weighted Symbolic Mutual Information (wSMI) measure (King *et al.*, 2013). This method calculates a non-linear index of information sharing between two signals. The signals are transformed into symbols. By defining a value of k, the number of samples that represent a symbol, and τ, the temporal separation between them, a frequency range is defined for which wSMI will be sensitized. The joint probability between the signals was then calculated for each pair of channels, for each trial, with a fixed value of k = 3 and τ = 32 ms—hence establishing the frequency range to 1–10 Hz. The

signals were low-pass filtered at 10 Hz to avoid aliasing effects (see Supplementary material for more details).

A seed analysis based on the wSMI was calculated for the amygdala's signal with the other regions within each subject for the intentional and unintentional conditions (signals without the baseline time window). The statistical comparisons between the connectivity values obtained for each condition were performed using a Wilcoxon Signed Rank test. The null hypothesis was rejected if a *t*-value was greater than the most extreme 5% of the distribution (i.e. $P < 0.05$). The BrainNet Viewer toolbox was used for visualization of wSMI.

Brief time span functional connectivity

A functional connectivity analysis (Omigie *et al.*, 2015) of the early window (0 to 500 ms) was implemented to study the correlation between different regions. The signals were first bandpass filtered in two frequency band ranges, 1 to 40 Hz and 60 to 150 Hz, for the intentional and unintentional signals. See Supplementary material for more details.

Results

During the task, we measured local field potentials (at T1, T2, and T3) in three patients (Subjects 1, 2 and 3) with depth electrodes ($n = 115$) placed in the amygdala (Fig. 1B, $n = 6$) and in several frontal, temporal and parietal locations ($n = 109$; see Supplementary Fig. 2 and Supplementary Table 2 for spatial locations).

Intentionality and content (harm versus neutral) were discriminated by an activity boost in the amygdala (all sites). This was observed during the first 200 ms after stimulus onset (T1) at 1–40 Hz and throughout T1–T2–T3 at broadband (60–150 Hz) (Fig. 1C and Supplementary Fig. 3). Bootstrapped permutations of single trial analysis revealed greater activity for intentional than unintentional harm at an early time window (80–200 ms, 1–40 Hz) and throughout the T1–T3 time points at broadband (Fig. 1D). This occurred separately in each patient (Supplementary Table 3).

Moreover, a trial-by-trial analysis of amygdala responses (averaged during T1–T3) at broadband predicted the subjects' subsequent categorization as intentional or unintentional (Fig. 1E). Such a classification was not predicted by the activity of any other region (Supplementary Fig. 4). The amygdala was the only site that systematically discriminated between critical conditions in all subjects (at both low and high bands) and predicted their classification of events.

To examine whether such modulation in the amygdala resonated in other regions, we analysed both (i) amygdala connections during the full stimulus set presentation; and (ii) connectivity at 1–40 Hz and broadband among all recording sites at early stages. First, via a wSMI analysis (King *et al.*, 2013), we explored the integration and global broadcasting of information across non-linear amygdala connections. At relatively low frequencies (1–10 Hz), enhanced fronto-amygdalar connectivity (each subject separately: Subject 1: mesial/lateral supplementary motor area; Subject 2: orbitofrontal cortex; Subject 3: inferior frontal gyrus, pars orbitalis, lateral and posterior medial frontal gyrus; Wilcoxon, threshold of $P < 0.05$) was observed for intentional relative to unintentional harm (Fig. 2A). The evoked responses of these prefrontal regions, which presented early connectivity with the amygdala, featured late (but not early) stimulus-related modulations (Supplementary Fig. 5). We also assessed functional connectivity among all recording sites at an early window (~T1: 0–500 ms). Again, compared with unintentional harm, intentional harm induced stronger frontotemporal connectivity in all patients (bootstrapping, for 1–40 Hz: Subject 1: $P = 6.3139 \times 10^{-35}$, $t = 42.54$; Subject 2: $P = 7.989 \times 10^{-33}$, $t = 35.24$; Subject 3: $P = 2.8841 \times 10^{-10}$, $t = 21.18$; for 60–150 Hz: Subject 1: $P = 5.2694 \times 10^{-48}$, $t = 42.35$; Subject 2: $P = 1.9606 \times 10^{-11}$, $t = 32.21$; Subject 3: $P = 2.7941 \times 10^{-58}$, $t = 43.95$, see Fig. 2B), even when controlling for the neutral condition (Supplementary Fig. 6). In addition, we found that intentional harm elicited increased fronto-temporal connectivity at medium and long range distances (Supplementary Fig. 7). Thus, detection of intentional harm was associated with greater fronto-amygdala information sharing during T1–T3 and with fronto-temporal coupling at early stages (~T1).

Discussion

Previous reports pointed to the amygdala as a critical hub to appraise intentional harmful actions and stimulus salience (Treadway *et al.*, 2014). Our results provide unprecedented spatiotemporal evidence for its role in the early encoding of intention, the subsequent categorization of harmful events, and the automatic modulation of corticolimbic connections. These findings support the view that the amygdala indexes the biological significance of salient stimuli through multi-pathway networks (Pessoa and Adolphs, 2010).

The concept of intentionality has been variously defined in the literature. Here, we propose that harm is intentional insofar as it reflects the perpetrator's motivation to deliberately hurt another person, leading to mostly negative moral judgements (Supplementary material). We have selected a well-validated and replicated set of stimuli allowing an early and unambiguous categorization of intentional harm versus unintentional harm, while controlling for basic variables (such as familiarity) (Supplementary material). Future studies should assess early modulations of amygdala activity by intentionality manipulating both basic variables and other potentially relevant cognitive dimensions (Supplementary material).

The amygdala has been implicated in the processing and transmission of sensory salient stimuli to guide behaviours and decision-making (Janak and Tye, 2015). Consistent with

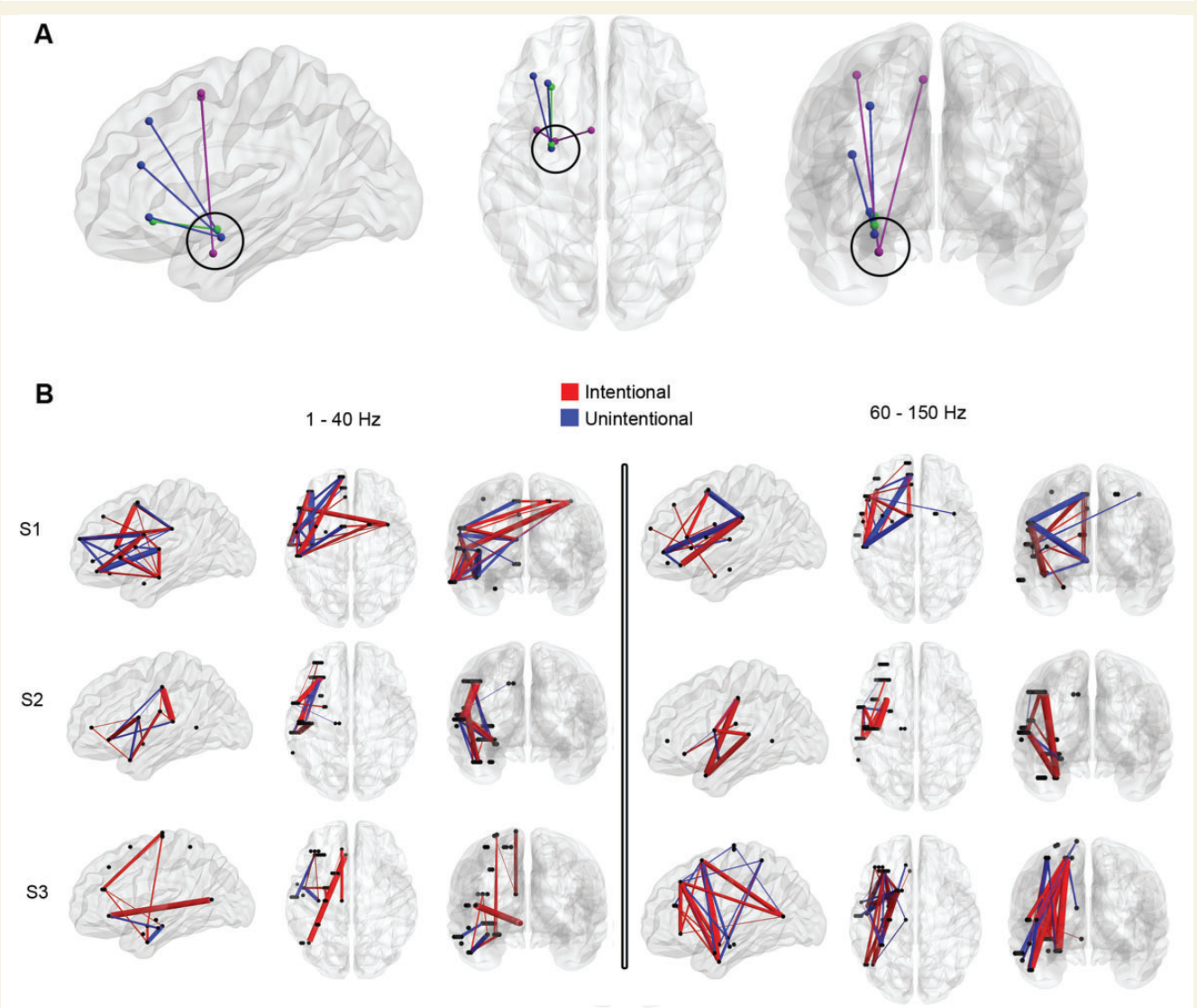

Figure 2 Corticolimbic and frontotemporal tuning of intentional actions. (**A**) WSMI. Significant connections of the amygdala with frontal regions for the intentional conditions (Wilcoxon Signed Rank Test, threshold of $P < 0.05$ for each subject). Each colour represents a different subject. (**B**) Brief Time Span Functional Connectivity. Significant correlations of intentional and unintentional conditions for each subject in a 0–500 ms window. Lines and line-widths indicate *t*-values and their absolute magnitudes, respectively. *Left*: A significantly larger number of connections (1–40 Hz) was found for the intentional conditions [$P < 0.01$ bootstrapping: Subject 1 (S1): $P = 6.3139 \times 10^{-35}$, $t = 42.54$; Subject 2 (S2): $P = 7.989 \times 10^{-33}$, $t = 35.24$; Subject 3 (S3): $P = 2.8841 \times 10^{-10}$,$t = 21.18$]. *Right*: A significantly larger number of connections (broadband) were found for the intentional conditions [Subject 1 (S1): $P = 5.2694 \times$ '10^{-48}, $t = 42.35$; Subject 2 (S2): $P = 1.9606 \times 10^{-11}$, $t = 32.21$; Subject 3 (S3): $P = 2.7941 \times 10^{-58}$, $t = 43.95$].

this claim, amygdala activity at broadband (a band that captures spike firing neurons) (Manning *et al.*, 2009) predicted single-trial behavioural performance, as previously reported for aversive learning (Lim *et al.*, 2009). The rapid (~125 ms) involvement of this structure replicates previous findings with scalp EEG (Decety and Cacioppo, 2012; Escobar *et al.*, 2014), highlighting its role in other automatic processes (Pessoa and Adolphs, 2010), such as emotional salience and face/object recognition (see Supplementary material for a deeper assessment of this finding). Note that relatively slow (Janak and Tye, 2015) and high (Oya *et al.*, 2002) amygdala frequencies are sensitive to stimulus salience modulations. The absence of similar discrimination/prediction in other associated regions corroborates the specificity of amygdala activity in intentionality attribution (Treadway *et al.*, 2014).

We also observed an early coupling of corticolimbic networks previously implicated in intentional harm processing (Treadway *et al.*, 2014) (Supplementary material). As detailed in the Supplementary material, this aligns with extant models of social cognition (Moll and Schulkin, 2009; Fumagalli and Priori, 2012; Ibanez and Manes, 2012) and fast fronto-amygdala networks (Pessoa and Adolphs, 2010). Using a novel method (wSMI) (King

et al., 2013), we showed enhanced information sharing at relatively slow (1–10 Hz) frequencies during observation of intentional actions. Because theta fronto-amygdaline oscillation is enhanced during aversive stimuli processing (Janak and Tye, 2015), this may indicate a general role for low-frequency coupling between these regions in the face of aversion-inducing events. Moreover, the early increases in frontotemporal connectivity suggest rapid spreading of amygdala boosts to other regions. Such a claim is consistent with the findings that (i) activity flows from limbic to frontal structures occur between 190–347 ms (Catenoix *et al.*, 2011); (ii) salient stimuli modulate cortical activity in early epochs (~100 ms) (Kawasaki *et al.*, 2001); causing (iii) parallel distributed frontotemporal processing (Krolak-Salmon *et al.*, 2004; Brazdil *et al.*, 2009) (Supplementary material).

Intracranial EEG recordings can provide novel and robust results (Foster *et al.*, 2015). Our results provide unprecedented spatiotemporal evidence for the role of amygdala in the early encoding of intention, the subsequent categorization of harmful events, and the automatic modulation of cortico-limbic connections, all systematically observed in each subject. Although intracranial measures provide a unique source of information that cannot be obtained through non-invasive methods, they also feature important limitations. We have carefully dealt with the well-known caveats of intracranial EEG research by adopting several precautions to minimize the effects of pathological tissue in our signals (Supplementary material). Finally, we could not presently examine laterality differences in amygdala activations, an issue that calls for further research (Supplementary material).

By overcoming the spatiotemporal limitations of previous neuroimaging studies of the amygdala, the present results help to clarify the 'many roads' view. Consistent with this perspective, we observed early amygdala responses guided by stimulus salience and rapid parallel coupling with other regions. Nevertheless, our results also highlight the amygdala's critical role in automatically encoding and classifying intentional harm during moral evaluation—functions that no other region seems to subserve.

Funding

This work was partially supported by grants from CONICET, CONICYT/FONDECYT Regular (1130920), FONCyT-PICT 2012-0412, 2012-1309, and the INECO Foundation. V.L. is sponsored by Fondecyt 1150241, M.S. is sponsored by CONICET and the James McDonnell Foundation 21st Century ScienceInitiative in Understanding Human Cognition Scholar Award.

Supplementary material

Supplementary material is available at *Brain* online.

References

Ames DL, Fiske ST. Perceived intent motivates people to magnify observed harms. Proc Natl Acad Sci USA 2015; 112: 3599–605.

Boubela RN, Kalcher K, Huf W, Seidel EM, Derntl B, Pezawas L, et al. fMRI measurements of amygdala activation are confounded by stimulus correlated signal fluctuation in nearby veins draining distant brain regions. Sci Rep 2015; 5: 10499.

Brazdil M, Roman R, Urbanek T, Chladek J, Spok D, Marecek R, et al. Neural correlates of affective picture processing–a depth ERP study. Neuroimage 2009; 47: 376–83.

Catenoix H, Magnin M, Mauguiere F, Ryvlin P. Evoked potential study of hippocampal efferent projections in the human brain. Clin Neurophysiol 2011; 122: 2488–97.

Decety J, Cacioppo S. The speed of morality: a high-density electrical neuroimaging study. J Neurophysiol 2012; 108: 3068–72.

Decety J, Cowell JM. The complex relation between morality and empathy. Trends Cogn Sci 2014; 18: 337–9.

Decety J, Michalska KJ, Kinzler KD. The contribution of emotion and cognition to moral sensitivity: a neurodevelopmental study. Cerebral Cortex. 2012; 22: 209–20.

Escobar MJ, Huepe D, Decety J, Sedeno L, Messow MK, Baez S, et al. Brain signatures of moral sensitivity in adolescents with early social deprivation. Sci Rep 2014; 4: 5354.

Foster BL, Rangarajan V, Shirer WR, Parvizi J. Intrinsic and task-dependent coupling of neuronal population activity in human parietal cortex. Neuron 2015; 86: 578–90.

Fumagalli M, Priori A. Functional and clinical neuroanatomy of morality. Brain 2012; 135(Pt 7): 2006–21.

Gross J. Analytical methods and experimental approaches for electrophysiological studies of brain oscillations. J Neurosci Methods 2014; 228: 57–66.

Huebner B, Dwyer S, Hauser M. The role of emotion in moral psychology. Trends Cogn Sci 2009; 13: 1–6.

Ibanez A, Cardona JF, Dos Santos YV, Blenkmann A, Aravena P, Roca M, et al. Motor-language coupling: direct evidence from early Parkinson's disease and intracranial cortical recordings. Cortex 2013; 49: 968–84.

Ibanez A, Manes F. Contextual social cognition and the behavioral variant of frontotemporal dementia. Neurology 2012; 78: 1354–62.

Jacobs J, Kahana MJ. Direct brain recordings fuel advances in cognitive electrophysiology. Trends Cogn Sci 2010; 14: 162–71.

Janak PH, Tye KM. From circuits to behaviour in the amygdala. Nature 2015; 517: 284–92.

Kawasaki H, Kaufman O, Damasio H, Damasio AR, Granner M, Bakken H, et al. Single-neuron responses to emotional visual stimuli recorded in human ventral prefrontal cortex. Nat Neurosci 2001; 4: 15–6.

King JR, Sitt JD, Faugeras F, Rohaut B, El Karoui I, Cohen L, et al. Information sharing in the brain indexes consciousness in noncommunicative patients. Curr Biol 2013; 23: 1914–9.

Krolak-Salmon P, Henaff MA, Vighetto A, Bertrand O, Mauguiere F. Early amygdala reaction to fear spreading in occipital, temporal, and frontal cortex: a depth electrode ERP study in human. Neuron 2004; 42: 665–76.

Lim SL, Padmala S, Pessoa L. Segregating the significant from the mundane on a moment-to-moment basis via direct and indirect amygdala contributions. Proc Natl Acad Sci USA 2009; 106: 16841–6.

Manning JR, Jacobs J, Fried I, Kahana MJ. Broadband shifts in local field potential power spectra are correlated with single-neuron spiking in humans. J Neurosci 2009; 29: 13613–20.

Moll J, Schulkin J. Social attachment and aversion in human moral cognition. Neurosci Biobehav Rev 2009; 33: 456–65.

Moll J, Zahn R, de Oliveira-Souza R, Krueger F, Grafman J. Opinion: the neural basis of human moral cognition. Nat Rev Neurosci 2005; 6: 799–809.

Naccache L, Gaillard R, Adam C, Hasboun D, Clemenceau S, Baulac M, et al. A direct intracranial record of emotions evoked by subliminal words. Proc Natl Acad Sci USA 2005; 102: 7713–7.

Omigie D, Dellacherie D, Hasboun D, George N, Clement S, Baulac M, et al. An intracranial EEG study of the neural dynamics of musical valence processing. Cereb Cortex 2015; 25: 4038–47.

Oya H, Kawasaki H, Howard MA, 3rd, Adolphs R. Electrophysiological responses in the human amygdala discriminate emotion categories of complex visual stimuli. J Neurosci 2002; 22: 9502–12.

Pessoa L, Adolphs R. Emotion processing and the amygdala: from a 'low road' to 'many roads' of evaluating biological significance. Nat Rev Neurosci 2010; 11: 773–83.

Treadway MT, Buckholtz JW, Martin JW, Jan K, Asplund CL, Ginther MR, et al. Corticolimbic gating of emotion-driven punishment. Nat Neurosci 2014; 17: 1270–5.

Tukey JW. Exploratory data analysis. Reading, MA: Addison-Wesley Pub. Co.; 1977.

Young L, Cushman F, Hauser M, Saxe R. The neural basis of the interaction between theory of mind and moral judgment. Proc Natl Acad Sci USA 2007; 104: 8235–40.

Supplementary Figures and Tables

Supplementary Figures

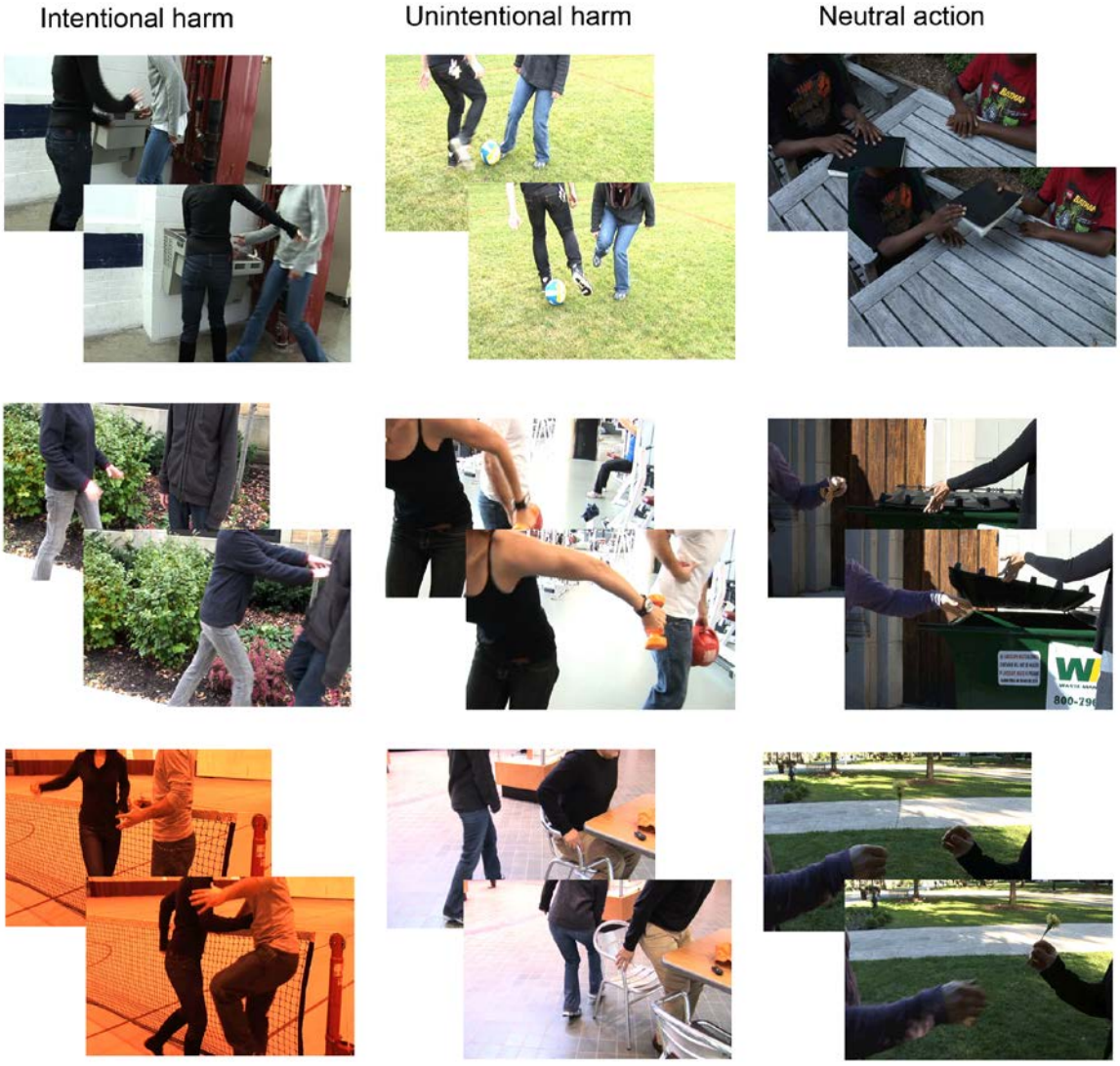

Supplementary Figure S1. Examples of stimuli depicting intentional, unintentional, and neutral conditions. Three examples in each column illustrate, from left to right, the first and third images of the sequence (T1 and T3) for intentional harm, unintentional harm, and neutral action.

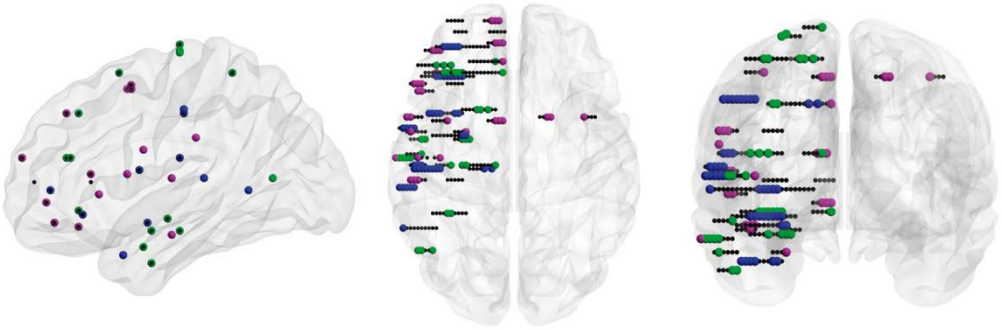

Supplementary Figure S2 Electrode contact sites for every subject. Each color represents a different subject (Magenta: subject 1, Blue: subject 2, Green: subject 3). Smaller black sites represent those electrodes that were discarded at the preprocessing stage (See **Preprocessing** section).

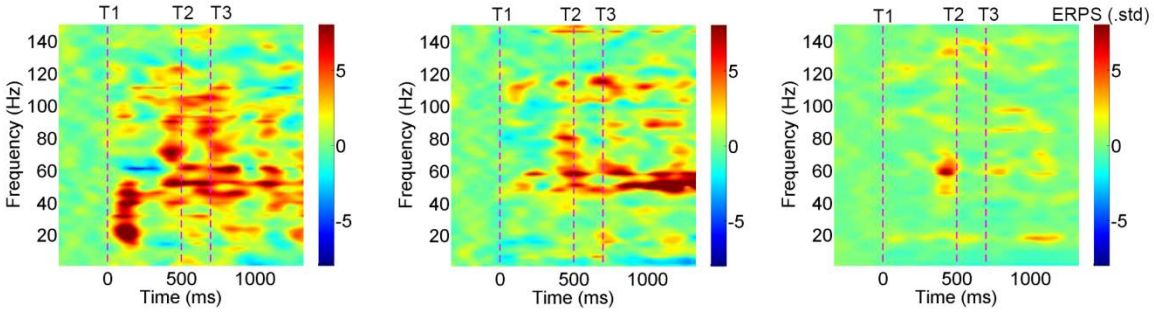

Supplementary Figure S3. Time-frequency charts for (from left to right) the intentional, unintentional, and neutral conditions of the averaged all of the amygdala's sites (statistical analyses are reported in Figure 1 and in the main text). T1, T2, and T3 represent the times at which each digital picture is presented to the participant.

	The region's averaged power for the intentional condition is not significantly different from its baseline and is not significantly larger from its averaged power for the unintentional condition.
	The amygdala's subtraction of its intentional and unintentional averaged power is significantly larger than the region's subtraction of the conditions' averaged power.
	The region's subtraction of its intentional and unintentional averaged power is equivalent to that of amygdala, but the region's logistic regression is not significant ($p<0.01$).
	The region's subtraction of its intentional and unintentional averaged power is significant ($p<0.01$), and the region's logistic regression is significant ($p<0.01$).

	Subject 1		Subject 2		Subject 3	
REGION	1 - 40 Hz	60 - 150 Hz	1 - 40 Hz	60 - 150 Hz	1 - 40 Hz	60 - 150 Hz
Amygdala						
Frontal						
Anterior Cingulate Cortex			N/A	N/A		
Posterior Cingulate Cortex	N/A	N/A			N/A	N/A
Posterior Orbital Gyrus	N/A	N/A			N/A	N/A
Anterior Superior Frontal Gyrus			N/A	N/A	N/A	N/A
Superior Frontal Gyrus			N/A	N/A	N/A	N/A
Mesial Mid Rostral Middle Frontal Gyrus	N/A	N/A	N/A	N/A		
Lateral Mid Rostral Middle Frontal Gyrus	N/A	N/A	N/A	N/A		
Posterior Rostral Middle Frontal Gyrus	N/A	N/A	N/A	N/A		
Middle Frontal Gyrus			N/A	N/A		
Inferior Frontal Sulcus	N/A	N/A			N/A	N/A
Inferior Frontal Gyrus - Pars Orbitalis			N/A	N/A		
Inferior Frontal Gyrus - Pars Triangularis					N/A	N/A
Inferior Frontal Gyrus - Pars Opercularis					N/A	N/A
Rolandic Operculum	N/A	N/A			N/A	N/A
Anterior Premotor - Frontal Mesial Gyrus			N/A	N/A	N/A	N/A
Anterior Premotor - Frontal Lateral Gyrus			N/A	N/A	N/A	N/A
Mesial Pre Supplementary Motor Area			N/A	N/A	N/A	N/A
Lateral Pre Supplementary Motor Area			N/A	N/A	N/A	N/A
Supplementary Motor Area	N/A	N/A	N/A	N/A		
Lateral Superior Precentral Gyrus	N/A	N/A	N/A	N/A		
Insular cortex						
Posterior Insula			N/A	N/A	N/A	N/A
Temporal						
Hippocampus	N/A	N/A	N/A	N/A		
Mesial Temporal Pole	N/A	N/A			N/A	N/A
Lateral Temporal Pole	N/A	N/A			N/A	N/A
Anterior Superior Temporal Gyrus			N/A	N/A		
Central Superior Temporal Gyrus						
Central Superior Temporal Sulcus	N/A	N/A			N/A	N/A
Anterior Middle Temporal Gyrus	N/A	N/A	N/A	N/A		
Central Middle Temporal Gyrus	N/A	N/A	N/A	N/A		
Lateral Middle Temporal Gyrus			N/A	N/A		
Anterior Superior Inferior Temporal Gyrus	N/A	N/A	N/A	N/A		
Posterior Inferior Temporal Gyrus	N/A	N/A			N/A	N/A
Parietal						
Superior Posterior Paracentral Lobule	N/A	N/A	N/A	N/A		
Poscentral Gyrus					N/A	N/A
Inferior Poscentral Gyrus	N/A	N/A			N/A	N/A
Lateral Anterior Superior Parietal Gyrus	N/A	N/A	N/A	N/A		

Supplementary Figure S4. Summary of the results for the color codes comparing the amygdala and the other regions in each subject for different frequency ranges over 0-200ms. Each color represents the tests with which the regions complied. Only 2 regions showed an early modulation at 1-40 Hz (intentional > unintentional, although logistic regression was non-significant), the ACC and OFG for one subject 1 only. Recent evidence

supports similar latencies in the frontal cortex similar to the earliest modulation of the amygdala (Pessoa and Adolphs, 2010).

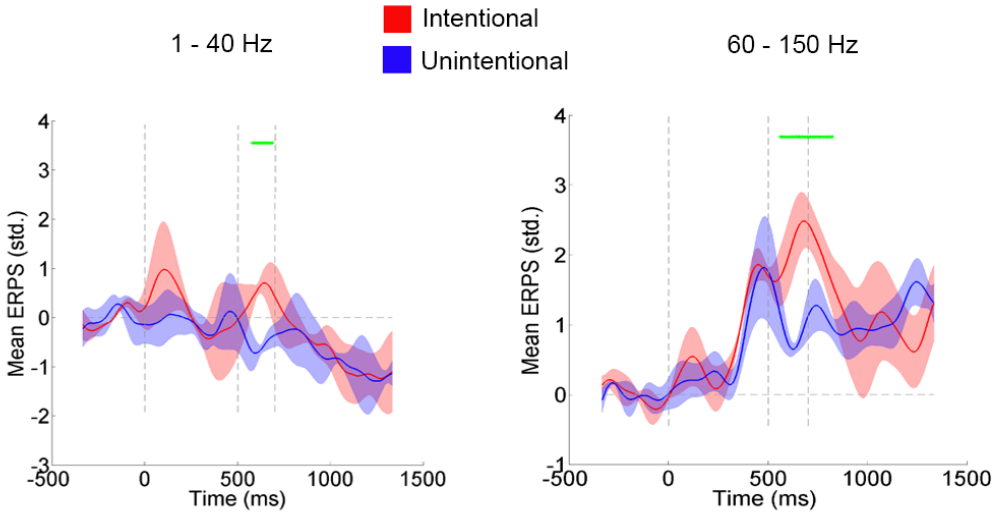

Supplementary Figure S5. Averaged power spectrum of the intentional and unintentional time-frequency charts using different frequency ranges (1-40 Hz and BB) for prefrontal cortex. The green marks identify significant differences between conditions (bootstrapping, $P < 0.01$). *Left*: Frequency range 1-40 Hz. *Right*: 60-150 Hz.

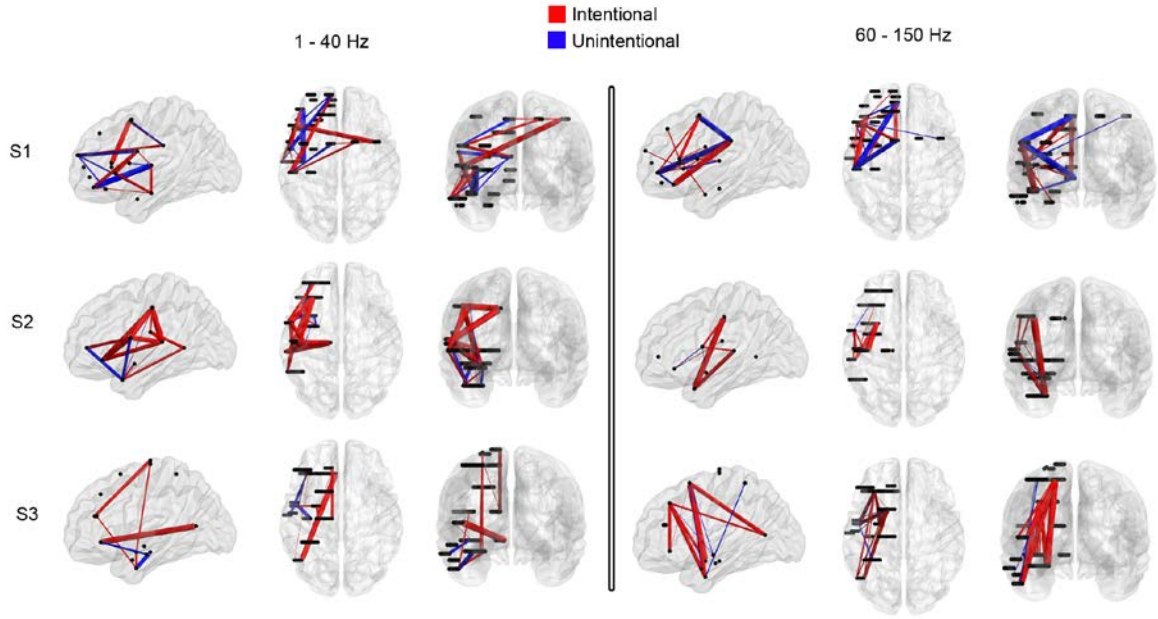

Supplementary Figure S6. Corticolimbic and frontotemporal tuning of intentional actions controlling by neutral condition. Brief Time Span Functional Connectivity. Significant correlations of intentional minus neutral and unintentional minus neutral conditions for each subject in a 0-500 ms window. Lines and line-widths indicate *t*-values and their absolute magnitudes, respectively. *Left*: A significantly larger number of connections (1-40Hz) was found for the intentional conditions (bootstrapping: S1: P= 1.9280 x 10^{-24}, t = 40.97; S2: P = 2.313 x 10^{-23}, t = 37.03; S3: P = 2.5236 x 10^{-11}, t 2 = 20.66). *Right*: A significantly larger number of connections (BB) were found for the intentional conditions (bootstrapping: S1: P= 1.2984 x 10^{-27}, t = 42.29; S2: P= 2.0966 x 10^{-23}, t = 37.20; S3: P= 6.6566 x 10^{-23}, t =35.47).

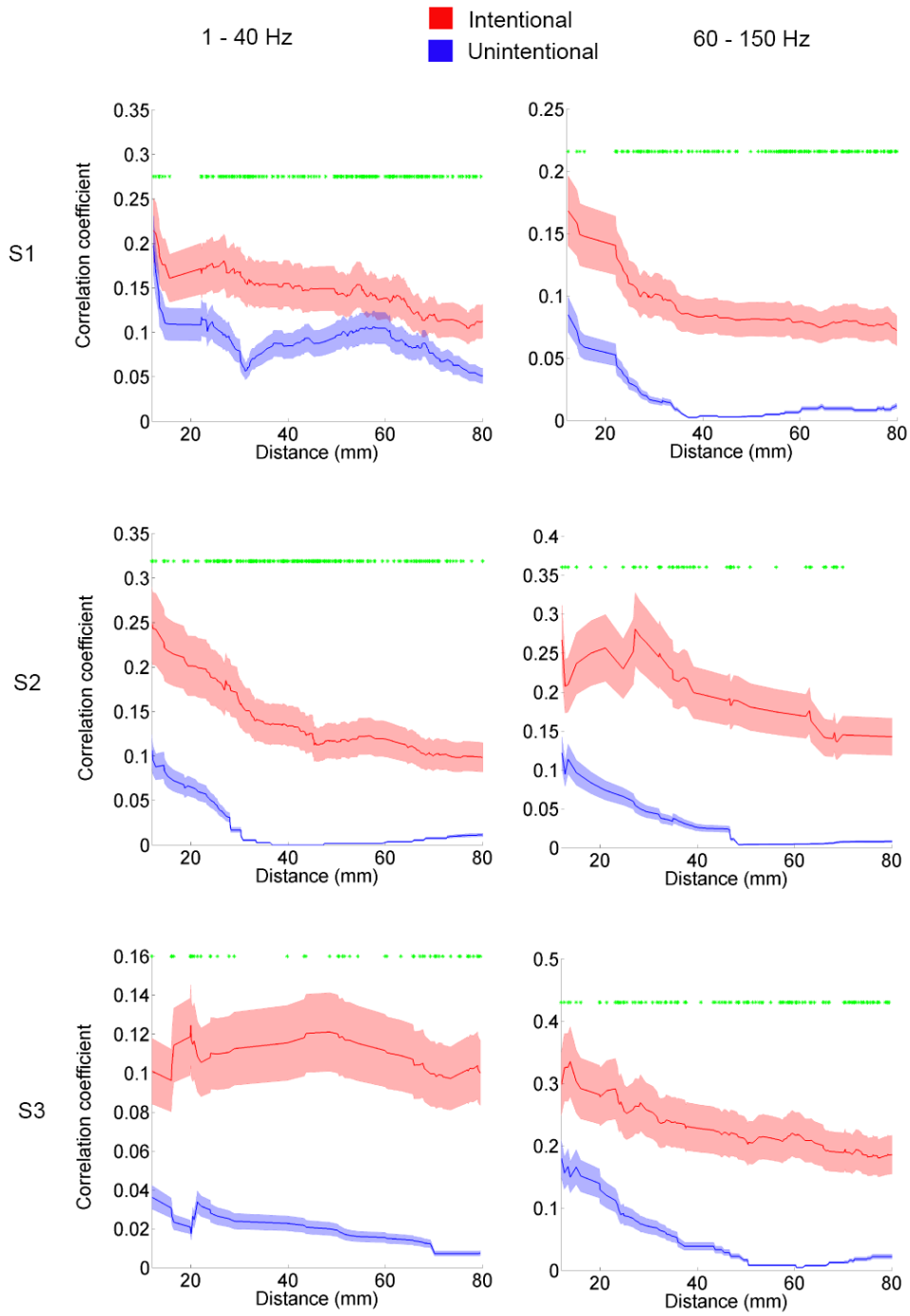

Supplementary Figure S7. Connectivity increase of intentional condition along Euclidean inter-electrode distances. *Left*: For each subject, significantly larger correlation coefficients for intentional condition were obtained for medium and long range distances for the frequency range of 1-40 Hz ($P < 0.01$). *Right:* For each subject,

significantly larger correlation coefficients for intentional condition were obtained for medium and long range distances for the frequency range 60-150 Hz ($P < 0.01$).

Supplementary Tables

Supplementary Table 1 Mean percentage of the accuracy and standard deviation by subject for the intentional and unintentional conditions.

	Intentional	**Unintentional**
Subject 1	86.36 % ± 6.43	72.73 % ±12.86
Subject 2	78.73 % ± 8.9	72.73 % ± 9.1
Subject 3	79.66 % ± 0	73.34 % ± 0

Supplementary Table 2. List of the recorded contact sites included in the analysis for each subject. MNI coordinates and Broadman regions are reported.

Subject	**Region**	**Electrode Label**	**Brodmann areas**	**X**	**y**	**Z**
1	Inferior Frontal Gyrus - Pars Orbitalis	OF'12	47	-42	32	-14
1	Anterior Cingulate Cortex	G'1	10	-6	48	-2
1	Anterior Cingulate Cortex	G'2	10	-8	48	-2
1	Anterior Cingulate Cortex	G'3	10	-10	48	-2
1	Inferior Frontal Gyrus - Pars Orbitalis	G'11	47	-40	44	-12
1	Inferior Frontal Gyrus - Pars Orbitalis	G'12	47	-42	44	-12
1	Inferior Frontal Gyrus - Pars Orbitalis	G'13	47	-44	44	-12
1	Middle Frontal Gyrus	GC'12	45	-50	26	12
1	Middle Frontal Gyrus	GC'13	45	-52	26	12
1	Middle Frontal Gyrus	GC'14	45	-54	26	12
1	Anterior Superior Frontal Gyrus	F'1	10	-8	60	20
1	Anterior Superior Frontal Gyrus	F'2	10	-10	60	20
1	Anterior Superior Frontal Gyrus	F'3	10	-12	60	20
1	Mesial Superior Frontal Gyrus	PM'1	32	-6	38	42
1	Lateral Pre Supplementary Motor Area	M'1	8	-6	6	54
1	Lateral Pre Supplementary Motor Area	M'2	8	-8	6	54
1	Lateral Pre Supplementary Motor Area	M'3	8	-10	6	54
1	Lateral Pre Supplementary Motor Area	M'11	8	-36	6	56
1	Inferior Frontal Gyrus - Pars Triangularis	OP'4	45	-50	22	2
1	Inferior Frontal Gyrus - Pars Triangularis	OP'5	45	-52	22	2
1	Mesial Supplementary Motor Area	M3	8	18	8	54
1	Mesial Supplementary Motor Area	M4	8	20	8	54
1	Anterior Premotor - Frontal Lateral Gyrus	M12	6	38	8	54

1	Inferior Frontal Gyrus - Pars Opercularis	R'4	6	-56	8	12
1	Inferior Frontal Gyrus - Pars Opercularis	R'5	6	-58	8	12
1	Poscentral Gryus	GP'13	48	-52	-26	30
1	Poscentral Gryus	GP'14	48	-54	-26	30
1	Poscentral Gryus	GP'15	48	-56	-26	30
1	Amygdala	A'1	34	-26	0	-22
1	Lateral Superior Temporal Gyrus	A'9	48	-56	0	24
1	Middle Temporal Gyrus	HP'8	22	-60	-14	-18
1	Middle Temporal Gyrus	HP'9	22	-62	-14	-18
1	Middle Temporal Gyrus	HP'10	21	-64	-14	-18
1	Insula Posterior	T'1	48	-40	-14	10
1	Superior Temporal Gyrus - Heschl's	T'5		-52	-14	10
2	Posterior Orbital Gyrus	OF4	47	-28	30	-8
2	Posterior Orbital Gyrus	OF5	47	-30	30	-8
2	Posterior Orbital Gyrus	OF6	47	-32	30	-8
2	Posterior Orbital Gyrus	OF7	47	-34	30	-8
2	Posterior Orbital Gyrus	OF8	47	-36	30	-8
2	Lateral Orbital Gyrus	OF9	47	-38	30	-8
2	Lateral Orbital Gyrus	OF10	47	-40	30	-8
2	Lateral Orbital Gyrus	OF11	47	-42	30	-8
2	Inferior Frontal Sulcus	GCA8	47	-30	46	4
2	Inferior Frontal Sulcus	GCA9	47	-32	46	4
2	Inferior Frontal Sulcus	GCA10	47	-34	46	4
2	Inferior Fontal Gyrus - Pars Triangularis	GCA11	47	-36	46	4
2	Inferior Fontal Gyrus - Pars Triangularis	GCA13	47	-38	46	4
2	Rolandic Operculum	R1	48	-54	2	14
2	Rolandic Operculum	R2	48	-56	2	14
2	Rolandic Operculum	R3	48	-58	2	14
2	Rolandic Operculum	R4	48	-60	2	14
2	Inferior Postcentral Gyrus	OP1	48	-50	-18	20
2	Inferior Postcentral Gyrus	OP3	48	-52	-18	20
2	Inferior Postcentral Gyrus	OP4	48	-54	-18	20
2	Posterior Cingulate Cortex	GCP1		-12	-20	42
2	Posterior Cingulate Cortex	GCP2		-16	-20	42
2	Postcentral Gyrus	GCP8	3	-40	-20	44
2	Postcentral Gyrus	GCP9	4	-42	-20	44
2	Postcentral Gyrus	GCP10	4	-44	-20	44
2	Postcentral Gyrus	GCP11	4	-46	-20	44
2	Postcentral Gyrus	GCP12	4	-48	-20	44
2	Postcentral Gyrus	GCP13	4	-50	-20	44
2	Postcentral Gyrus	GCP14	4	-52	-20	44
2	Postcentral Gyrus	GCP15	3	-54	-20	44
2	Mesial Temporal Pole	PT1	38	-30	10	-28
2	Mesial Temporal Pole	PT3	38	-32	10	-28
2	Lateral Temporal Pole	PT7	20	-40	10	-28
2	Lateral Temporal Pole	PT8	20	-42	10	-28
2	Lateral Temporal Pole	PT9	20	-44	10	-28
2	Lateral Temporal Pole	PT10	20	-46	10	-28
2	Amygdala	A2	34	-26	-2	-12
2	Amygdala	A3	34	-28	-2	-12
2	Central Superior Temporal Sulcus	T1	22	-54	-30	10
2	Central Superior Temporal Sulcus	T2	22	-56	-30	10
2	Central Superior Temporal Sulcus	T3	22	-58	-30	10
2	Central Superior Temporal Sulcus	T4	22	-60	-30	10
2	Central Superior Temporal Sulcus	T5	22	-62	-30	10
2	Posterior Inferior Temporal Gyrus	FS10	21	-60	-52	4
2	Posterior Cingulate Cortex	GCP1		-12	-20	42
3	Anterior Cingulate Cortex	OF'1	11	-6	32	-6
3	Inferior Frontal Gyrus - Pars Orbitalis	OF'6	47	-28	32	-6
3	Inferior Frontal Gyrus - Pars Orbitalis	OF'7	47	-30	32	-6
3	Inferior Frontal Gyrus - Pars Orbitalis	OF'8	47	-32	32	-6
3	Inferior Frontal Gyrus - Pars Orbitalis	OF'9	47	-34	32	-6
3	Inferior Frontal Gyrus - Pars Orbitalis	OF'10	47	-36	32	-6
3	Inferior Frontal Gyrus - Pars Orbitalis	OF'11	47	-38	32	-6
3	Anterior Cingulate	GC'1	32	-10	38	20
3	Mesial Mid Rostral Middle Frontal Gyrus	GC'6	46	-34	36	20

3	Lateral Mid Rostral Middle Frontal Gyrus	GC'8	45	-38	36	20
3	Lateral Mid Rostral Middle Frontal Gyrus	GC'10	45	-42	36	20
3	Posterior Rostral Middle Frontal Gyrus	F'8	9	-30	32	42
3	Posterior Rostral Middle Frontal Gyrus	F'9	9	-32	32	42
3	Supplementary Motor Area	M'1	6	-14	12	62
3	Central Middle Frontal Gyrus	M'5	6	-18	12	62
3	Central Middle Frontal Gyrus	M'6	8	-20	12	62
3	Superior Posterior Paracentral Lobule	PC'1	6	-10	-18	76
3	Lateral Superior Precentral Gyrus	PC'6	6	-26	-18	73
3	Lateral Superior Precentral Gyrus	PC'7	6	-28	-18	72
3	Lateral Anterior Superior Parietal Gyrus	AS'5	2	-34	-44	62
3	Lateral Anterior Superior Parietal Gyrus	AS'6	2	-36	-44	62
3	Lateral Posterior Middle Temporal Gyrus	PI'1	37	-44	-64	10
3	Lateral Posterior Middle Temporal Gyrus	PI'4	37	-50	-64	10
3	Lateral Posterior Middle Temporal Gyrus	PI'5	37	-52	-64	10
3	Superior Central Middle Temporal Gyrus	I'51	22	-50	-12	-10
3	Anterior Middle Temporal Gyrus	T1'1	21	-56	0	-24
3	Hippocampus	H'1	20	-34	-18	-16
3	Central Middle Temporal Gyrus	H'6	20	-56	-14	-18
3	Central Middle Temporal Gyrus	H'7	20	-58	-14	-18
3	Central Middle Temporal Gyrus	H'8	21	-60	-14	-18
3	Central Middle Temporal Gyrus	H'9	21	-62	-14	-18
3	Amygdala	A'1	34	-24	-4	-16
3	Amygdala	A'2	34	-26	-4	-16
3	Amygdala	A'3	34	-28	-4	-16

Supplementary Table 3. Time windows of the significant differences in each subject for the Intentional>Unintentional comparison using bootstrapped permutations for 1-40 Hz in an early time window (0-200 ms) and for 60-150 Hz (BB) along T1 to T3.

	1 - 40 Hz (0-200ms)	**60-150 Hz (T1-T2-T3)**
Subject 1	80-227ms	102-126ms and 696-704ms
Subject 2	88-227ms	80-100ms, 177-327ms, 495-662ms and 813-872ms
Subject 3	98-35ms	629-713ms

REFERENCES

Pessoa L, Adolphs R. Emotion processing and the amygdala: from a 'low road' to 'many roads' of evaluating biological significance. Nature reviews Neuroscience 2010; 11(11): 773-83.

Supplementary Data

1. Stimuli validation

The task we used in this study was designed years ago and employed in several neuroimaging (fMRI, high-density EEG) studies with adult participants (including forensic populations) and children (Decety and Cacioppo, 2012; Decety *et al.*, 2012; Harenski *et al.*, 2012; Escobar *et al.*, 2014; Yoder and Decety, 2014a, b; Decety *et al.*, 2015). The stimuli have been recently adapted to assess neurodynamic and behavioral (eye-tracking) responses to intentional harm in babies and pre-school children (Cowell and Decety, 2015a; Cowell and Decety, 2015b). Here we refer to three publications (Decety and Cacioppo, 2012; Decety *et al.*, 2012; Escobar *et al.*, 2014) to describe how the stimuli were created and validated.

The stimuli were initially validated on computerized visual analog scales for perceived intentionality and empathic concern by a group of 26 participants aged between 18 and 23. Eye-tracking and pupillary dilatation data were simultaneously recorded with a Tobii T120 system. Results showed that subjective ratings of empathic concern were higher for intentional than unintentional harm sequences ($F(1, 100) = 300.59$; $P < 0.001$). Participants' pupil dilations were analyzed with repeated-measures ANOVA. A main effect of intentionality ($F(1, 25) = 30.46$; $P < 0.001$) revealed larger pupil dilation in response to clips depicting intentional harm.

In another study (17 healthy participants, 39% female, mean age: 21.86; $SD = 3.13$), we showed that participants could distinguish intentional from unintentional harm with 90% accuracy ($P < 0.05$) (Decety and Cacioppo, 2012).

2. Additional stimuli validation

2.1. Intentionality, aggression, and empathic concern

Before the study, intentional and unintentional stimuli were also validated on computerized visual analog scales by a group of 40 participants. In an independent experiment, we asked them to assess each clip in terms of intentionality –from 1 (unintentional) to 5 (intentional)– aggressiveness –from 1 (low aggression) to 5 (high aggression)–, and empathic concern –from 1 (low empathic concern) to 5 (high empathic concern). Intentional harmful actions were classified as more intentional than unintentional ones [$F(1, 38) = 30.46$; $P < 0.001$; intentional = 4.23 ($SD = 1.62$); unintentional = 1.8, ($SD = 1.85$)]. The levels of aggression depicted in the intentional ($M = 4.3$, $SD = 1.35$) and unintentional ($M = 3.8$, $SD = 1.68$) conditions were statistically similar ($F(1, 38) = 3.42$; $P = .23$). The subjective ratings of empathic concern with stimuli depicting harm were higher for intentional ($M = 4.64$, $SD = 1.72$) than unintentional ($M = 2.11$, $SD = 1.21$; $F(1, 38) = 23.42$; $P < 0.001$) situations. This is expected, given that harmful actions perceived as intentional are automatically classified as more harmful and elicit enhanced empathic concern, even when the ensuing harm is identical in both conditions (the 'intent-magnifies-harm' effect) (Ames and Fiske, 2013, 2015).

2.2. T1: Stimulus categorization, intention to harm, harm level, and stimulus properties.

Finally, note that early effects were observed at T1 both here and in previous reports (e.g., Escobar *et al.*, 2014). We thus analyzed the stimulus categorization, the ratings of intention to harm, the level of harm, and the stimulus properties at T1 (first slide). We asked 41 participants (female: 48%, mean age: 28, $SD = 2.7$; mean educational level: 15, $SD = 6.4$) to classify the stimuli in three categories: intentional harm, unintentional harm, and neutral. Regarding stimulus categorization (SC), we found good levels of accuracy at this window (intentional: $M = 81\%$, $SD = 2.4$; unintentional: $M = 79\%$, $SD = 2.4$; neutral: $M = 82\%$, $SD = 2.4$; with no difference among conditions: $F(2, 80) = 1.05$, $P = 0.35$).

Then we asked the participants to rate the stimuli in terms of intention to harm –from 1 (totally unintentional) to 10 (totally intentional)–, level of harm –from 1 (not harmful at all) to 10 (totally harmful)–, familiarity –from 1 (not familiar at all) to 10 (totally familiar)–,

and ambiguity of the depicted situation –from 1 (totally ambiguous) to 10 (totally unambiguous).

We found a significant effect of intention to harm ($F(2, 80) = 85.15$, $P=0.0001$). Post hoc comparisons (Tukey's HSD test; $MSE = 1.74$, $df = 80$) showed that perceived intentionality was higher in the intentional ($M = 8.60$, $SD = 0.77$) than in the unintentional ($M = 4.92$, $SD = 0.82$, $P<0.01$) or the neutral ($M = 1.09$, $SD = 0.84$, $P<0.01$) conditions. Regarding harm, a significant effect was also observed ($F(2, 80) = 78.09$, $P<0.01$). Post hoc comparisons (Tukey's HSD test; $MSE = 1.99$, $df = 80$) revealed that the intentional condition ($M = 7.81$, $SD = 0.57$) elicited higher levels of harm than unintentional ($M = 6.30$, $SD = 0.87$, $P<0.05$) and neutral ($M = 1.21$, $SD = 0.81$, $P<0.01$) conditions. The unintentional condition also yielded increased levels of harm relative to the neutral condition ($P<0.01$). No significant effects were observed for familiarity ($F(2, 80) = 0.98$, $P=0.37$; intentional = 7.4, $SD = 1.21$; unintentional = 7.01, $SD = 0.98$; neutral = 6.9, $SD = 0.93$) or ambiguity ($F(2, 80) = 0.06$, $P=0.94$; intentional = 7.41, $SD = 1.54$; unintentional = 7.08, $SD = 1.82$; neutral = 8.01, $SD = 1.93$).

To evaluate which factors (model one: intention to harm and harm; model two: familiarity and ambiguity) drives the subjects' initial categorization of stimuli (SC of intentional harm scenarios and unintentional harm scenarios), we built two multiple regression models of the stimulus categorization (SC, percentage of accuracy). In the first model, ratings of intention to harm and harm were entered as predictors of the stimulus categorization. This allowed us to evaluate the effects of each predictor (intention to harm and harm) while controlling the other. This model ($F(4, 36) = 8.16$, $P < 0.01$, $R2 = 0.37$) showed that intention to harm (but not harm) was the only predictor ($\beta = 0.66$, $\eta^2 = 0.25$) of subjects' categorizations. Nevertheless, when controlling for the effect of intentionality, harm itself did not predict the subjects' categorization ($\beta = -0.06$, $\eta^2 = 0.04$). This confirmed that subjects' categorization (at T1) was driven by differences in the degree of intentionality and not by harm level itself, supporting the intent-magnifies-harm effect (Ames and Fiske, 2013, 2015). Moreover, in the second model, neither familiarity ($\beta = -0.06$, $\eta^2 = 0.04$) nor

ambiguity (β = -0.06, η^2 = 0.04) predicted the subjects' categorization ($F(4, 36) = 2.13$, $P > 0.05$, $R2 = 0.11$).

3. Comparison between the amygdala and the other regions

Step 1. Using bootstrapping methods, statistical comparisons were performed between the baseline values and a time window of values between 0 to 200 ms for frequency ranges of 1 to 40 Hz and 60 to 150 Hz. This analysis was performed for the intentional condition and the subtraction between the intentional and unintentional conditions. It included every region, grouped by ROI, for each subject. Its purpose was to evaluate whether the region discriminates the intentional condition, and the intentional from unintentional conditions. Statistical significance was considered to be $p<0.01$.

Step 2. Using bootstrapping methods, statistical comparisons were performed between the subtraction of the intentional and unintentional conditions of the amygdala and the other regions, grouped by ROI, for each subject for the frequency band ranges of 1 to 40 Hz and 60 - 150 Hz for time values between 0 to 200 milliseconds. Statistical significance was considered to be $p<0.01$. This was performed to compare the amygdala's power activation with that of the regions that did discriminate the intentional conditions and the intentional from unintentional conditions.

Step 3. For regions whose mean power was not significantly smaller than that of the amygdala, we performed a logistic regression of single trial. The parameters used were described earlier.

4. Amygdalar connectivity analysis using Weighted Symbolic Mutual Information (WSMI)

WSMI is calculated between each pair of channels, for each trial, and the signal is then transformed into a series of discrete symbols. It assesses the extent to which the two signals present joint nonrandom fluctuations, suggesting that they share information. It has three main advantages: (i) it allows for a rapid and robust estimation of the signals' entropies; (ii)

it provides an efficient way to detect non-linear coupling; and (iii) it discards the spurious correlations between signals arising from common sources, favoring non-trivial pairs of symbols (King *et al.*, 2013).

The signals were first transformed into a series of discrete symbols that were defined by the ordering of k time samples separated by a temporal separation τ. The analysis was restricted to a fixed symbol size (k = 3, that is, 3 samples represent a symbol) and τ = 32 ms between samples (temporal distance between samples), which determines a frequency range coverage of 1-10 Hz. Low-pass filters at 10 Hz were used to avoid aliasing artifacts. WSMI was estimated using a joint probability matrix multiplied by the binary weights. These weights were set to zero for pairs of (a) identical symbols and (b) opposed symbols that could be elicited by a unique common source.

5. Brief Time Span Functional Connectivity

Pearson's correlation test was then used between the signals of different regions within each subject for the time samples corresponding to 0-500 milliseconds. We consider that a subject has n recordings (one for each contact site), as denoted by $x_i(t)$, where i is the number of contact sites within the subject (i = 1,2,...,n) and t indicates the sampled time within an epoch (t = 1,2,...,T). The functional connectivity matrix between region i and region j is defined as Pearson's correlation coefficient between $x_i(t)$ and $x_j(t)$:

$$C_{ij} = \frac{\sum_{t=1}^{T}(x_i(t)-\bar{x_i})(x_j(t)-\bar{x_j})}{\sqrt{\sum_{t=1}^{T}(x_i(t)-\bar{x_i})^2}\sqrt{\sum_{t=1}^{T}(x_j(t)-\bar{x_j})^2}} \quad ,$$

The mean value of $x_i(t)$ is given by

$$\bar{x_i} = \left(\frac{1}{T}\right)\sum_{t=1}^{T} x_i(t) \quad .$$

The statistical comparisons between the correlation values obtained for each condition were performed using bootstrapping as described above. The BrainNet Viewer toolbox was also used for visualization purposes.

In order to quantify the networks' characterization and compare between intentional and unintentional conditions, we calculated a function correlation considering the Euclidean distance between each pair of electrodes (King *et al.,* 2013) and then performed statistical analysis using bootstrapping, as previously described.

To control for the neutral condition, we performed the same analysis, except that the neutral condition matrix was subtracted from the intentional condition and unintentional condition matrices. The resulting matrices were then statistically compared following the same method previously reported.

REFERENCES

Ames DL, Fiske ST. Intentional harms are worse, even when they're not. Psychological science 2013; 24(9): 1755-62.

Ames DL, Fiske ST. Perceived intent motivates people to magnify observed harms. Proceedings of the National Academy of Sciences of the United States of America 2015; 112(12): 3599-605.

Cowell J, Decety J. Precursors to morality in development: A complex interplay between neural, socio-environmental, and behavioral facets. Proceedings of the National Academy of Sciences 2015a; In press.

Cowell JM, Decety J. The neuroscience of implicit moral evaluation and its relation to generosity in early childhood. Current biology : CB 2015b; 25(1): 93-7.

Decety J, Cacioppo S. The speed of morality: a high-density electrical neuroimaging study. J Neurophysiol 2012; 108(11): 3068-72.

Decety J, Chen C, Harenski CL, Kiehl KA. Socioemotional processing of morally-laden behavior and their consequences on others in forensic psychopaths. Hum Brain Mapp 2015; 36(6): 2015-26.

Decety J, Michalska KJ, Kinzler KD. The contribution of emotion and cognition to moral sensitivity: a neurodevelopmental study. Cereb Cortex 2012; 22(1): 209-20.

Escobar MJ, Huepe D, Decety J, Sedeno L, Messow MK, Baez S, *et al.* Brain signatures of moral sensitivity in adolescents with early social deprivation. Scientific reports 2014; 4(5354).

Harenski CL, Thornton DM, Harenski KA, Decety J, Kiehl KA. Increased frontotemporal activation during pain observation in sexual sadism: preliminary findings. JAMA Psychiatry 2012; 69(3): 283-92.

King JR, Sitt JD, Faugeras F, Rohaut B, El Karoui I, Cohen L, *et al*. Information sharing in the brain indexes consciousness in noncommunicative patients. Current biology : CB 2013; 23(19): 1914-9.
Yoder KJ, Decety J. The Good, the bad, and the just: justice sensitivity predicts neural response during moral evaluation of actions performed by others. J Neurosci 2014a; 34(12): 4161-6.
Yoder KJ, Decety J. Spatiotemporal neural dynamics of moral judgment: a high-density ERP study. Neuropsychologia 2014b; 60: 39-45.

Supplementary Discussion

1. Intentionality and intentional harm

In the domain of moral cognition, intentional harm is generally proposed to reflect the motivation of the action's perpetrator. Detecting whether an action was intentional or unintentional and assessing its consequences is critical to pass moral judgment and to determine the severity of punishment (Ames and Fiske, 2013, 2015). This capacity develops very early in ontogeny. Young infants (8 months) rely on intentionality as a cue to determine moral relevance (Hamlin, 2013). Also, numerous neuroimaging and behavioral studies with adults support the view that intentionality judgments both precede and guide moral cognition (e.g.,(Young *et al.*, 2007; Cushman, 2008; Decety and Cacioppo, 2012; Decety *et al.*, 2012)). Moreover, our validation study (Supplementary Data section 2) shows that the intention to harm (and not the level of harm proper) triggers the classification of stimuli –in agreement with the finding that adult moral judgment is determined primarily by the ascribed intention (Cushman, 2008; Young and Saxe, 2009). This pattern follows the widely described "harm magnification effect" (Darley and Pittman, 2003; Ames and Fiske, 2013, 2015), which shows that people overestimate intentional harm, assigning more blame, punishment, and moral condemnation to their peprpetrators. Besides, we also controlled for other potential confounders. The stimuli had similar levels of familiarity and ambiguity (see Supplementary Data section 2), and the protagonists' faces were not visible to avoid emotional bias. On the other hand, most previous reports using intracranial recordings assessed iERPs or oscillations without assessing whether brain modulations predict single-trial classification during task performance. We showed that trial-by-trial amygdalar activity was closely related to single-trial behavioral classification of stimuli as intentional/unintentional. Moreover, we have statistically compared the activity of the amygdala (both activity and prediction of subjects' classification during the task) with many other fronto-temporal regions. In each subject, the amygdala was the only site that systematically discriminated between the critical conditions and predicted when events were classified as intentional or unintentional. Thus, these control factors support the specific sensitivity of the amygdala to intentional harm. However, and despite these methodological precautions and specific results, our main findings should be further

tested and expanded via different paradigms. Future assessments should determine whether other relevant variables such as ambiguity/familiarity, emotional clues, and different classes of intentional harm are in turn interacting with the early amygdalar and cortico-limbic network activation.

2. Early effects in the amygdala

The heightened saliency of intentional harm relies on understanding both the motivation of the perpetrator and the consequences of the action. Early amygdalar activation in the face of relevant stimuli may be an accurate correlate. These early effects, though somewhat surprising, have been consistently observed for different types of stimuli. In human intracranial recordings of the amygdala, the processing of faces/emotions elicited neural activations at 40-200 ms (Oya *et al.*, 2002; Krolak-Salmon *et al.*, 2004; Pessoa and Adolphs, 2010; Pourtois *et al.*, 2010; Sato *et al.*, 2011; Meletti *et al.*, 2012). In monkeys, intracranial recordings of the amygdala during visual discrimination revealed activation at 60-300 ms latencies (Leonard *et al.*, 1985; Nakamura *et al.*, 1992). MEG studies of face/object processing showed amygdalar responses at 100-250 ms (Cornwell *et al.*, 2008). Previous EEG studies with similar tasks requiring classification of intentional harm reported early processing at ~100 ms (Escobar *et al.*, 2014). EEG/MEG studies also show very early modulation of salient stimuli at ~70-100 ms for emotional valence (Redcay and Carlson, 2015), at 70 ms for pain (Senkowski *et al.*, 2011), and at 55-90 ms for the discrimination of different stimulus properties (Ramkumar *et al.*, 2013); as well as typical modulations by salient stimuli at 90 ms (Lachat *et al.*, 2012). Even the processing of high-level cognitive processes, such as semantic discrimination, have shown an earlier activation at 40-60 ms (Palva *et al.*, 2002) and at 50-80 ms after stimulus onset for affective associative learning (Rehbein *et al.*, 2014). Thus, our results are in agreement with this evidence and congruent with the rapid automatic detection of intentional harmful actions, arguably needed for survival.

As the frequency analysis is window-centered, we consider that the earliest unbiased significant temporal value is around 125 ms, when the window center is at 0 ms (T1 stimulus presentation). Frequency calculations are performed using a centered sliding window. That is, when the window is centered at a given time point t a temporal

segment ranging from t-125 ms to t+125 ms (125 ms being half the window length) is used to determine the signal's frequency components. When t = 0 ms (T1 stimulus presentation), the signal used for frequency calculation ranges from 125 ms at baseline to 125 ms post-stimulus. We consider that the earliest unbiased significant temporal value is around 125 ms when only the post-stimulus signal is used to calculate the frequency spectrum. Since the epochs were baseline-corrected, it is still possible to consider previous (< 125 ms) unbiased significant temporal values given that the baseline should not account for spectrum obtained (as the baseline signal should be close to 0 μV). Nonetheless, following a more conservative position, our claims about temporal significance are restricted to values after 125 ms.

3. Prefrontal cortex modulation

As the amygdala and the prefrontal cortex are regions associated with the processing of harmful stimuli (Decety *et al.*, 2012; Treadway *et al.*, 2014), and they showed stronger connectivity in our study, we also performed a time-frequency analysis of these prefrontal regions. The earliest time points at which its activity differs for each condition are 580 ms for 1-40 Hz and 570 ms for BB. This may reflect a lag of the amygdala's differential activity, probably triggered by enhanced connectivity during intentional harm. Thus, the functional connectivity analysis performed in the 0-500 ms time window suggest that the prefrontal cortex is sharing information with the amygdala at early latencies. This is consistent with other studies that show an amygdalar-prefrontal coupling in early time windows. Human intracranial stimulation studies have reported connectivity between paralimbic structures and the prefrontal cortex at earlier latencies (Catenoix *et al.*, 2005; Catenoix *et al.*, 2011). Intracranial recordings in monkeys show that attended stimuli enhance long-range connectivity at very early latencies (110-160 ms) (Gregoriou *et al.*, 2009). Similarly, different MEG/EEG studies of semantic processing (Bedo *et al.*, 2014), perceptual binding (Rodriguez *et al.*, 1999), interoception (Canales-Johnson *et al.*, 2015), and somatosensory processes (Hu *et al.*, 2012) have found similar or even earlier couplings than those presently reported.

4. Relevance for theoretical models of moral cognition

Drawing on previous fMRI studies which included functional connectivity analyses (Decety *et al.*, 2012; Treadway *et al.*, 2014) and high-density EEG measures (Decety and Cacioppo, 2012; Escobar *et al.*, 2014), we speculate that the amygdala may signal the early detection of intentional harm and then relay this information to prefrontal networks to guide social decision-making, including moral evaluation, judgment (ventromedial prefrontal cortex), and punishment (dorsolateral prefrontal cortex). Moreover, previous works show that the functional connectivity between the amygdala and prefrontal cortex show increased coupling when individuals perceive intentional harm in comparison to unintentional harm (Decety *et al.*, 2012), specially for punishment of intentional harm (Treadway *et al.*, 2014). Thus, our results integrate (a) the proposed frontotemporal networks involved in moral cognition (Moll and Schulkin, 2009; Fumagalli and Priori, 2012) with (b) the early processing of frontotemporal coupling, and (c) empirical (Ames and Fiske, 2013, 2015) and theoretical (Hauser and Wood, 2010) accounts which indicate the foundational role that judgments of intentionality play in human social cognition and, more particularly, in moral cognition.

5. Limitations and further assessment

Intracranial recordings occur exceptionally in humans and provide a unique opportunity to analyze brain function with high temporal and spatial resolution. In the present study, recordings were obtained from patients suffering from pharmacologically intractable epilepsy, which means that they may not accurately represent a healthy population (Tukey, 1977). To account for that, we followed recent reports from cognitive neuroscience research (Dastjerdi *et al.*, 2013; Parvizi *et al.*, 2013; Foster *et al.*, 2015) and controlled for relevant factors. First, similar recording sites typically include multiple pathological and healthy brain regions (Musch *et al.*, 2014). We addressed this issue by: (i) excluding channels in epileptic focus regions, (ii) using stringent inclusion criteria for the remaining channels (see Signal Preprocessing subsection)(Manning *et al.*, 2009), (iii) carefully inspecting MRI scans to rule out structural abnormalities, and (iv) including only patients with relatively normal cognitive function as measured by neuropsychological tests (Oya *et al.*, 2002). The replication of results across patients

(Shum *et al.*, 2013) suggests that despite the limitations our conclusions are well-founded. As shown in previous reports (Dastjerdi *et al.*, 2013; Foster *et al.*, 2015), intracranial EEG recordings of three subjects can provide novel and robust results when they offer exceptional data and control of the above factors. Moreover, none of the subjects in our study presented epileptic activity in their amygdalae. Indeed, epileptogenic foci were distant from such a structure. Also, epileptogenic activity was absent in many other frontotemporal regions (Subject 1: 35 sites; Subject 2: 44 sites; Subject 3: 36 sites; all after the exclusion of 194 electrodes following stringent criteria). These conditions are very infrequent. In fact, we obtained recordings from several patients over three years to be able to find three subjects meeting the criteria described above. Thus, although we cannot avoid the intrinsic limitations of intracranial recordings, we have controlled for the most influential and recognized confounds.

We could not presently examine laterality differences in amygdalar activations, an issue that calls for further research. Recent studies suggest that the left amygdala is implicated in the determination of intentional cooperation (Singer *et al.*, 2004), consequential damage and agent intent (Yu *et al.*, 2015), in-group harm (Molenberghs *et al.*, 2014), harm avoidance and stimulus valence interaction (Van Schuerbeek *et al.*, 2014), rapid orientation to masked fearful faces (Carlson *et al.*, 2009), reactive aggression associated with anatomical anomalies (Bobes *et al.*, 2013), moral and social transgressions in presence of an audience (Finger *et al.*, 2006) and the modulation of the perceived agency by a social context on the perception of pain (Akitsuki and Decety, 2009). However, other neuroimaging studies showed right amygdala engagement in the generation and regulation of unpleasant emotions (Kohno *et al.*, 2015), processing of negative emotional images (Lungu *et al.*, 2015), and empathy-related brain responses to dynamic fearful faces (Toller *et al.*, 2015). Moreover, intracranial recordings of right amygdala showed an early effect of gaze (Huijgen *et al.*, 2015) and induced coupled oscillations in response to painful laser stimulations (Liu *et al.*, 2015).

Most of the above studies have at least two drawbacks: (i) they were performed using neuroimaging techniques, which are not good indicators of laterality given the inherent noise level and signal artifact; and (ii) none of them advanced specific hypotheses on laterality. Lesion studies are important to determine laterality effects. Left amygdala lesions impair auditory cortical processing of vocal emotions (Fruhholz *et al.*, 2015) and

emotional facilitation of interference resolution (Levens *et al.*, 2011). On the other hand, lesion studies show that the right amygdala can influence the retention of complex emotional stimuli (Edith Frank and Tomaz, 2003) and it is predisposed to process aversive emotions (Angrilli *et al.*, 1996; Labudda *et al.*, 2014). Thus, left and right functional roles of the amygdala in the detection of intentional harm and related stimuli are not clear. Future studies with intracranial recordings from right (and, ideally, bilateral) amygdalae might be able to elucidate laterality effects involved in the detection of intentional harm.

REFERENCES

Akitsuki Y, Decety J. Social context and perceived agency affects empathy for pain: an event-related fMRI investigation. NeuroImage 2009; 47(2): 722-34.

Ames DL, Fiske ST. Intentional harms are worse, even when they're not. Psychological science 2013; 24(9): 1755-62.

Ames DL, Fiske ST. Perceived intent motivates people to magnify observed harms. Proceedings of the National Academy of Sciences of the United States of America 2015; 112(12): 3599-605.

Bedo N, Ribary U, Ward LM. Fast dynamics of cortical functional and effective connectivity during word reading. PloS one 2014; 9(2): e88940.

Bobes MA, Ostrosky F, Diaz K, Romero C, Borja K, Santos Y, *et al.* Linkage of functional and structural anomalies in the left amygdala of reactive-aggressive men. Social cognitive and affective neuroscience 2013; 8(8): 928-36.

Canales-Johnson A, Silva C, Huepe D, Rivera-Rei A, Noreika V, Garcia MD, *et al.* Auditory Feedback Differentially Modulates Behavioral and Neural Markers of Objective and Subjective Performance When Tapping to Your Heartbeat. Cereb Cortex 2015; 21.

Carlson JM, Reinke KS, Habib R. A left amygdala mediated network for rapid orienting to masked fearful faces. Neuropsychologia 2009; 47(5): 1386-9.

Catenoix H, Magnin M, Guenot M, Isnard J, Mauguiere F, Ryvlin P. Hippocampal-orbitofrontal connectivity in human: an electrical stimulation study. Clin Neurophysiol 2005; 116(8): 1779-84.

Catenoix H, Magnin M, Mauguiere F, Ryvlin P. Evoked potential study of hippocampal efferent projections in the human brain. Clin Neurophysiol 2011; 122(12): 2488-97.

Cornwell BR, Carver FW, Coppola R, Johnson L, Alvarez R, Grillon C. Evoked amygdala responses to negative faces revealed by adaptive MEG beamformers. Brain research 2008; 1244: 103-12.

Cushman F. Crime and punishment: distinguishing the roles of causal and intentional analyses in moral judgment. Cognition 2008; 108(2): 353-80.

Darley JM, Pittman TS. The psychology of compensatory and retributive justice. Personality and social psychology review : an official journal of the Society for Personality and Social Psychology, Inc 2003; 7(4): 324-36.

Dastjerdi M, Ozker M, Foster BL, Rangarajan V, Parvizi J. Numerical processing in the human parietal cortex during experimental and natural conditions. Nature communications 2013; 4: 2528.

Decety J, Cacioppo S. The speed of morality: a high-density electrical neuroimaging study. J Neurophysiol 2012; 108(11): 3068-72.
Decety J, Michalska KJ, Kinzler KD. The contribution of emotion and cognition to moral sensitivity: a neurodevelopmental study. Cereb Cortex 2012; 22(1): 209-20.
Escobar MJ, Huepe D, Decety J, Sedeno L, Messow MK, Baez S, *et al*. Brain signatures of moral sensitivity in adolescents with early social deprivation. Scientific reports 2014; 4(5354).
Finger EC, Marsh AA, Kamel N, Mitchell DG, Blair JR. Caught in the act: the impact of audience on the neural response to morally and socially inappropriate behavior. NeuroImage 2006; 33(1): 414-21.
Foster BL, Rangarajan V, Shirer WR, Parvizi J. Intrinsic and task-dependent coupling of neuronal population activity in human parietal cortex. Neuron 2015; 86(2): 578-90.
Fumagalli M, Priori A. Functional and clinical neuroanatomy of morality. Brain : a journal of neurology 2012; 135(Pt 7): 2006-21.
Gregoriou GG, Gotts SJ, Zhou H, Desimone R. High-frequency, long-range coupling between prefrontal and visual cortex during attention. Science 2009; 324(5931): 1207-10.
Hamlin JK. Failed attempts to help and harm: intention versus outcome in preverbal infants' social evaluations. Cognition 2013; 128(3): 451-74.
Hauser M, Wood J. Evolving the capacity to understand actions, intentions, and goals. Annu Rev Psychol 2010; 61: 303-24.
Hu L, Zhang ZG, Hu Y. A time-varying source connectivity approach to reveal human somatosensory information processing. NeuroImage 2012; 62(1): 217-28.
Krolak-Salmon P, Henaff MA, Vighetto A, Bertrand O, Mauguiere F. Early amygdala reaction to fear spreading in occipital, temporal, and frontal cortex: a depth electrode ERP study in human. Neuron 2004; 42(4): 665-76.
Lachat F, Farroni T, George N. Watch out! Magnetoencephalographic evidence for early modulation of attention orienting by fearful gaze cueing. PloS one 2012; 7(11): e50499.
Leonard CM, Rolls ET, Wilson FA, Baylis GC. Neurons in the amygdala of the monkey with responses selective for faces. Behav Brain Res 1985; 15(2): 159-76.
Manning JR, Jacobs J, Fried I, Kahana MJ. Broadband shifts in local field potential power spectra are correlated with single-neuron spiking in humans. The Journal of neuroscience : the official journal of the Society for Neuroscience 2009; 29(43): 13613-20.
Meletti S, Cantalupo G, Benuzzi F, Mai R, Tassi L, Gasparini E, *et al*. Fear and happiness in the eyes: an intra-cerebral event-related potential study from the human amygdala. Neuropsychologia 2012; 50(1): 44-54.
Molenberghs P, Gapp J, Wang B, Louis WR, Decety J. Increased Moral Sensitivity for Outgroup Perpetrators Harming Ingroup Members. Cereb Cortex 2014.
Moll J, Schulkin J. Social attachment and aversion in human moral cognition. Neurosci Biobehav Rev 2009; 33(3): 456-65.
Musch K, Hamame CM, Perrone-Bertolotti M, Minotti L, Kahane P, Engel AK, *et al*. Selective attention modulates high-frequency activity in the face-processing network. Cortex; a journal devoted to the study of the nervous system and behavior 2014; 60: 34-51.
Nakamura K, Mikami A, Kubota K. Activity of single neurons in the monkey amygdala during performance of a visual discrimination task. J Neurophysiol 1992; 67(6): 1447-63.

Oya H, Kawasaki H, Howard MA, 3rd, Adolphs R. Electrophysiological responses in the human amygdala discriminate emotion categories of complex visual stimuli. The Journal of neuroscience : the official journal of the Society for Neuroscience 2002; 22(21): 9502-12.
Palva S, Palva JM, Shtyrov Y, Kujala T, Ilmoniemi RJ, Kaila K, *et al.* Distinct gamma-band evoked responses to speech and non-speech sounds in humans. The Journal of neuroscience : the official journal of the Society for Neuroscience 2002; 22(4): RC211.
Parvizi J, Rangarajan V, Shirer WR, Desai N, Greicius MD. The will to persevere induced by electrical stimulation of the human cingulate gyrus. Neuron 2013; 80(6): 1359-67.
Pessoa L, Adolphs R. Emotion processing and the amygdala: from a 'low road' to 'many roads' of evaluating biological significance. Nature reviews Neuroscience 2010; 11(11): 773-83.
Pourtois G, Spinelli L, Seeck M, Vuilleumier P. Temporal precedence of emotion over attention modulations in the lateral amygdala: Intracranial ERP evidence from a patient with temporal lobe epilepsy. Cognitive, affective & behavioral neuroscience 2010; 10(1): 83-93.
Ramkumar P, Jas M, Pannasch S, Hari R, Parkkonen L. Feature-specific information processing precedes concerted activation in human visual cortex. The Journal of neuroscience : the official journal of the Society for Neuroscience 2013; 33(18): 7691-9.
Redcay E, Carlson TA. Rapid neural discrimination of communicative gestures. Social cognitive and affective neuroscience 2015; 10(4): 545-51.
Rehbein MA, Steinberg C, Wessing I, Pastor MC, Zwitserlood P, Keuper K, *et al.* Rapid plasticity in the prefrontal cortex during affective associative learning. PloS one 2014; 9(10): e110720.
Rodriguez E, George N, Lachaux JP, Martinerie J, Renault B, Varela FJ. Perception's shadow: long-distance synchronization of human brain activity. Nature 1999; 397(6718): 430-3.
Sato W, Kochiyama T, Uono S, Matsuda K, Usui K, Inoue Y, *et al.* Rapid amygdala gamma oscillations in response to eye gaze. PloS one 2011; 6(11): e28188.
Senkowski D, Kautz J, Hauck M, Zimmermann R, Engel AK. Emotional facial expressions modulate pain-induced beta and gamma oscillations in sensorimotor cortex. The Journal of neuroscience : the official journal of the Society for Neuroscience 2011; 31(41): 14542-50.
Shum J, Hermes D, Foster BL, Dastjerdi M, Rangarajan V, Winawer J, *et al.* A brain area for visual numerals. The Journal of neuroscience : the official journal of the Society for Neuroscience 2013; 33(16): 6709-15.
Singer T, Kiebel SJ, Winston JS, Dolan RJ, Frith CD. Brain responses to the acquired moral status of faces. Neuron 2004; 41(4): 653-62.
Treadway MT, Buckholtz JW, Martin JW, Jan K, Asplund CL, Ginther MR, *et al.* Corticolimbic gating of emotion-driven punishment. Nature neuroscience 2014; 17(9): 1270-5.
Tukey JW. Exploratory data analysis. Reading, Mass.: Addison-Wesley Pub. Co.; 1977.
Van Schuerbeek P, Baeken C, Luypaert R, De Raedt R, De Mey J. Does the amygdala response correlate with the personality trait 'harm avoidance' while evaluating emotional stimuli explicitly? Behavioral and brain functions : BBF 2014; 10: 18.
Young L, Cushman F, Hauser M, Saxe R. The neural basis of the interaction between theory of mind and moral judgment. Proceedings of the National Academy of Sciences of the United States of America 2007; 104(20): 8235-40.

Young L, Saxe R. Innocent intentions: a correlation between forgiveness for accidental harm and neural activity. Neuropsychologia 2009; 47(10): 2065-72.
Yu H, Li J, Zhou X. Neural substrates of intention--consequence integration and its impact on reactive punishment in interpersonal transgression. The Journal of neuroscience : the official journal of the Society for Neuroscience 2015; 35(12): 4917-25.